GEOPHYSICAL RESEARCH LETTERS, VOL. 14, NO. 8, PAGES 840-843, AUGUST 1987

M_m : USE OF A VARIABLE-PERIOD MANTLE MAGNITUDE FOR THE RAPID ONE-STATION ESTIMATION OF TELESEISMIC MOMENTS

Jacques Talandier[1], Dominique Reymond[1] and Emile A. Okal[2]

Abstract. Broadband records of the first passage of Rayleigh waves at Papeete, Tahiti from large circum-Pacific earthquakes are used to recover in real time their seismic moments. The magnitude concept is used at periods varying from 50 to 300 s. Adequate corrections are made for distance and period. Typical standard deviations are 0.2 orders of magnitude on M_0. This mantle scale M_m can be extended continuously with no additional corrections over 4 orders of magnitude. It can be measured in the frequency- or time-domains, and we describe briefly the automation of the method, with obvious applications in tsunami warning.

Introduction

Thanks to the recent development of broadband seismometer systems with large dynamic range, it is now possible to routinely obtain high quality records of the first passage R_1 of ultra-long period Rayleigh waves in the 100 to 300 s period range, even from the largest teleseismic events. Figure 1 is a typical example of such a record, obtained at Papeete, Tahiti [PPT], following the 1985 Mexican earthquake.

Ultra-long period signals can be used to retrieve the seismic moment of the event in the lowest-frequency part of the spectrum, which itself controls the tsunami potential of the earthquake, when the latter takes place at sea. There are several advantages to the use of R_1 as opposed to subsequent passages. Because of its shorter travel time, R_1 is less affected by lateral heterogeneity, and thus more reliable for the retrieval of earthquake source parameters [Monfret and Romanowicz, 1986]. Also, and again simply because it arrives sooner, R_1 has the potential for the earlier issuance of a tsunami watch or warning.

The present paper discusses the real time estimation of M_0 through the use of a low-frequency magnitude scale, M_m, based on the measurement of mantle Rayleigh waves at a variable period, and such that

$$M_m = \log_{10} M_0 - 20 \qquad (1)$$

where M_0 is in dyn-cm. A companion paper [Okal and Talandier, 1987; hereafter Paper 1] has established the theoretical background justifying this approach, and explicited M_m as

$$M_m = \log_{10} X(\omega) + C_D + C_S - 0.90 \qquad (2)$$

where $X(\omega)$ is the spectral amplitude of R_1 at angular frequency ω, measured in μm-s, C_D a distance correction, and C_S a source excitation correction; both corrections are frequency dependent.

[1]Laboratoire de Géophysique, C.E.A., Boîte Postale 640, Papeete, Tahiti
[2]Department of Geological Sciences, Northwestern University, Evanston, Illinois 60201

Paper number 7L7180.
0094-8276/87/007L-7180$03.00

In the present endeavor, we are guided by several goals. First, we wish to develop a one-station method; this is a legitimate concern even in the day of instant satellite communications, especially so in the case of tsunami danger from relatively close-by events (e.g., in the Tonga-to-Tahiti geometry). Secondly, we remain guided by the magnitude concept: rather than attempting to solve for all components of the moment tensor, we aim at obtaining the scalar value of M_0; indeed, we have shown [Okal, 1985] that focal geometry (except in loose sediments) and source depth (at least in the 10—75 km range where most catastrophic Pacific earthquakes occur) are only moderate contributors to tsunami excitation. Similarly, we showed in Paper 1 that depth largely loses its influence over Rayleigh excitation at periods over 40 s, and that the use of a variable period can guard against the possible effect of the station sitting in a node of radiation, at least for a non-pure focal geometry.

Measurements of M_m

Instrumentation and Dataset

The dataset for this study consists of broadband records obtained at PPT since 1973. The response of this system (operated since 1972) is flat in displacement from 1 s to 150 s and decreases by a factor $\sqrt{2}$ at 300 s. As a first dataset, we concentrate on the 20 large earthquakes listed in Table 1, which occurred at distances $\Delta = 23$—85° from PPT, and have published moments over 10^{27} dyn-cm (over 3×10^{27} before 1979). These values are taken primarily from the CMT Harvard datasets; other sources are listed on Table 1.

Method

For each event, a 4096-point digital time series (with a sampling rate of 0.2 s) is Fourier-transformed, and at each period $T = 2\pi/\omega \geq 50$ s, the spectral amplitude $X(\omega)$ retained. The distance correction C_D contains the geometrical spreading factor $\log \sqrt{\sin\Delta}$ and the frequency dependent correction for anelastic attenuation. The latter takes into account regional variations in group velocity and Q.

A frequency-dependent correction C_S is then applied to compensate for the variation of surface wave excitation with T. Paper 1 has justified the expression

$$C_S = 2.0398\,\theta^3 - 1.3122\,\theta^2 + 0.39342\,\theta + 3.9335 \qquad (3)$$

where $\theta = \log_{10} T - 1.7657$, resulting from theoretical computations of the excitability of Rayleigh waves, averaged over all possible focal geometries, and over depth in the interval $h = 10$—75 km. It would be inappropriate only at higher frequencies, or if the station sits in a node of radiation. In order to at least partially remedy the latter situation, we evaluate magnitudes at all FFT periods between 50 and 300 s, and retain their largest value as the final M_m. The Appendix describes the automation of these measurements.

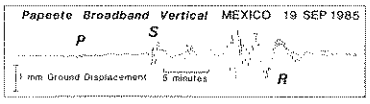

Fig. 1. Papeete broadband record of Event 17.

Results

Table 1 lists the "raw" values of M_m computed from Eqn. (2) for the 20 events in our dataset and compares them to the theoretical values expected from published moments. The best-fitting regression of $\log_{10}M_0$ against M_m has a slope $\alpha = 0.83$; the closeness of this number to 1 upholds the proportionality of $X(\omega)$ to M_0. With α constrained to 1, the mean and standard deviation of the residual r between measured and computed values of M_m are $\bar{r} = 0.18$; $\sigma = 0.16$. The latter corresponds to an uncertainty of a multiplicative or divisive factor f of 1.44 on the seismic moment (which we write as $f = */1.44$). Our results are also shown on Figure 2. We regard them as generally excellent. First, it should be remembered that individual estimates of seismic moments published by different investigators regularly show deviations on the order of $*/1.3$. Also, in the case of conventional magnitude scales (e.g., M_s at 20 s), few single seismic stations can boast of having a systematic magnitude bias of less than 0.2 units, and a standard deviation also less than 0.2 units. Our systematic bias $\bar{r}$ may be due to the procedure of retaining the largest magnitude values; we attempted to eliminate it by retaining the average, rather than the largest, value of M_m in the 50—300 s period range; this was unsuccessful, resulting in $\bar{r} = -0.08$ but $\alpha = 0.79$ and $f = */1.57$, a significant deterioration of the fit.

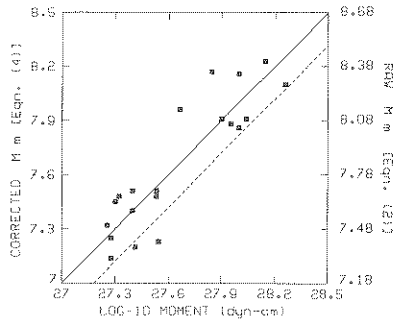

Fig. 2. Measured M_m against published M_0. The individual dots are the values of M_m listed in Table 1. If referred to the right axis, they represent the raw values; if referred to the left axis, they are the final, corrected values. The solid and dashed lines follow the theoretical relation $M_m = \log_{10}M_0 - 20$, for the final and raw values, respectively.

Test of Additional Corrections for Cornered Spectra.

As mentioned in Paper 1, Eqn. (2) applies only if the measurement is taken on the flat portion of the seismic spectrum, at a frequency lower than the first corner frequency of the source. For our largest events, this may not always be true. We first approach this problem by restricting the periods at which M_m is measured to 100 s and longer. This reduces $\bar{r}$ to 0.15, but decreases α to 0.74 and increases f to $/*1.58$, again a deterioration of the general fit of the data.

A second approach is to use an additional correction, for those events showing a cornered spectrum. Following Paper 1, we take $C_{CF} = \log(\pi \tau_s / T)$, where τ_s

TABLE 1. Values of M_m measured in this study

Number	Date	Epicentral Region	Distance to PPT (°)	Published Moment (10^{27} dyn-cm)	Equivalent M_m	Source †	Measured M_m Raw Eq. (2)	Final Eq. (4)	Period (s)	TD (corr.)
1	17 Jun 73	Japan	85	7.	7.85	a	8.35	8.17	273	8.04
2*	03 Oct 74	Peru	69	18.	8.26	b	8.28	8.10	164	8.26
3*	22 Jun 77	Tonga	25	14.	8.15	c	8.41	8.23	102	8.31
4	12 Jun 78	Japan	85	3.4	7.53		7.66	7.48	273	7.31
5	29 Nov 78	Mexico	62	3.5	7.54		7.41	7.23	205	7.28
6	28 Feb 79	Alaska	78	1.9	7.28		7.32	7.14	102	7.29
7*	14 Feb 79	Mexico	59	1.8	7.26		7.50	7.32	205	7.31
8	08 Jul 80	Santa Cruz	43	2.1	7.32		7.66	7.48	205	7.52
9*	17 Jul 80	Santa Cruz	43	8.	7.90		8.09	7.91	205	8.04
10	06 Jul 81	Vanuatu	37	2.6	7.41		7.38	7.20	82	7.12
11	01 Sep 81	Samoa	23	1.9	7.28		7.43	7.25	273	6.78
12	19 Dec 82	Tonga	25	2.	7.30		7.63	7.45	273	7.57
13*	26 May 83	Japan	88	4.6	7.66		8.14	7.96	164	8.00
14*	04 Oct 83	Chile	73	3.4	7.53		7.69	7.51	205	7.63
15	07 Feb 84	Solomon	49	2.5	7.40		7.69	7.51	59	7.69
16*	03 Mar 85	Chile	70	10.	8.00		8.04	7.86	164	8.05
17*	19 Sep 85	Mexico	58	11.	8.04		8.09	7.91	205	7.82
18*	21 Sep 85	Mexico	59	2.5	7.40		7.58	7.40	205	7.60
19*	07 May 86	Aleutian	72	10.	8.00	d	8.34	8.16	205	8.24
20	20 Oct 86	Kermadec	27	9.	7.95	e	8.06	7.88	51	7.98

† Moment sources: a, Shimazaki [1974]; b, Kanamori [1977]; c, Talandier and Okal [1979]; d, Ekström and Dziewonski [1986]; e, B.A. Romanowicz [pers. comm., 1987]; otherwise Harvard CMT dataset.

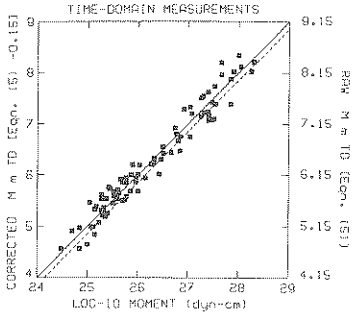

Fig. 3. Same as Figure 2 for the time-domain measurements of M_m. The correction applied to Eqn. (5) to refer the data to the left scale is -0.15 magnitude units.

is the source duration. Guided by the Harvard CMT dataset, we first take a constant $\tau_s = 35$ s; we apply this correction to 10 events whose spectra suggest a corner frequency in our frequency range (asterisk in Table 1). Resulting M_m values computed from Eqn. (8) of Paper 1 yield $\bar{r} = 0.21$; $f = */1.49$, again a deterioration of the fit. We also explored the possibility of τ_s varying with M_0, as predicted by scaling laws [e.g., Geller, 1976]. We tested values of M_m computed from Eqn. (7) of Paper 1, and found $\bar{r} = 0.30$; $f = */1.62$, again providing no improvement in the fit.

In conclusion, neither of these attempts improves the quality of fit of the residuals r substantially. This probably reflects the fact that the largest value of M_m, retained by our algorithm, is most often taken at extremely long periods (typically between 100 and 300 s; see "Period" column of Table 1). Thus, Eqn. (2), once corrected by the ad hoc constant 0.18

$$M_m = \log_{10} X(\omega) + C_D + C_S - 1.08 \qquad (4)$$

provides the most satisfactory fit to the dataset. Table 1 lists the final M_m values, after correction. The left scale and solid line in Figure 2 show the fit of the corrected data to the published values of M_0.

Time-Domain Measurements

It has long been known that there exists a theoretical relationship between M_0 and the spectral amplitude $X(\omega)$ of a Rayleigh wave; however most magnitude measurements have traditionally been taken in the time domain. On the basis of the strong inverse dispersion of Rayleigh waves in the 50—300 s period range, we discussed in Paper 1 a theoretical relationship of the form $X(\omega) = a \cdot T/2$ where a is the zero-to-peak amplitude of a time-domain oscillation of period T, within a strongly dispersed wavetrain. This in turn suggests the direct measurement of M_m in the time domain using

$$M_m^{TD} = \log_{10}(a \cdot T) + C_D + C_S - 1.20 \qquad (5)$$

where a is in μm, and T in s. We tested that possibility by measuring the amplitudes and periods of the arches making up the dispersed Rayleigh wave, and retaining the largest value of M_m^{TD} computed through (5). The Appendix describes the automation of this measurement for large earthquakes.

The residuals of M_m^{TD} versus the published values lead to $\bar{r} = 0.22$; $f = */1.67$. If Eqn. (5) is corrected by the same constant (–0.18) as Eqn. (2), the residual is only $\bar{r} = 0.04$. The quality of this result is in itself remarkable, given the crudeness of the approximations which led to propose (5) in Paper 1; however, the magnitude of Event 11 (Samoa, 1981) is grossly underestimated by this method. The last column in Table 1 lists the values obtained from the 20 earthquakes in our dataset, after this correction is made.

Extension to Smaller Events

In this section, we extend the above measurements to an additional dataset of 68 earthquakes with published moments between 5×10^{24} and 3×10^{27} dyn-cm. Spectral measurements were taken for 16 events ($M_0 > 3 \times 10^{26}$), and time-domain measurements for the entire dataset.

For the total dataset of 36 events with spectral determinations of M_m ($M_m = 6.5$—8.2), and using Eqn. (4), we obtain $\alpha = 1.06$, and when the slope is constrained to 1, $\bar{r} = 0.07$; $f = */1.57$.

Time domain measurements were taken visually (using pencil and ruler) on all 88 events, using Eqn. (5), although for the smaller events, the period at which M_m is taken was usually between 20 and 35 s. This dataset, shown on Figure 3 and spanning nearly four units of M_m, resulted in $\alpha = 0.98$, and when the slope is constrained to 1, $\bar{r} = 0.15$; $f = */1.67$. It should not be surprising that a good fit can be obtained between the time-domain visual measurements of M_m and $\log_{10} M_0$ for the smaller events, since this is simply an example of the relationship between moment and magnitude in the absence of saturation effects. (although the accuracy of C_S for the smaller events, most of which involve measurements at periods between 20 and 35 s, could be questionable). It is remarkable however (i) that the corrections required to Eqns. (2) (0.18) and (5) (0.15) are practically identical, and (ii) that the same "locking" constants can be used in Eqn. (5) over four orders of magnitudes, and with periods ranging from 20 to 270 s. This character of universality at all periods is the most important and promising feature of the mantle magnitude scale M_m.

Conclusions

1. Single station measurements on very-low frequency Rayleigh waves recorded by broad-band instruments, give reliable estimates of teleseismic moments in the range 10^{26} to 10^{28} dyn-cm. In this frequency range (3.5 to 20 mHz), source finiteness corrections C_{CF} are not warranted.

2. The only departure from the theoretical formula derived in Paper 1 is the subtraction of the constant 0.18 in Eqn. (4). This may be due to the procedure of taking the largest value of M_m in a range of periods. It may also be regarded as a "station correction"; further work using other stations (e.g., from the GEOSCOPE net) will address this matter.

3. The more easily taken time-domain measurements show no significant difference with frequency domain estimations, and thus uphold experimentally the crude approximation justifying their use. Again, the fit is improved significantly by subtracting 0.15 from Eqn. (5). Time domain measurements can even be extended down to $M_0 = 5 \times 10^{24}$ dyn-cm, while keeping the same constants in the Eqn. (5) defining M_m.

4. The final challenge will of course be the correct

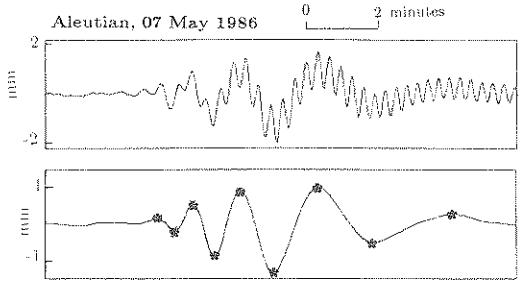

Fig. A-1. Principle of automatic determination of time-domain magnitude: *Top:* Original record of Event 19 at PPT. *Bottom:* Same record after filtering out periods greater than 50 s. The stars indicate the automatic picks of peaks and troughs, from which the amplitudes and periods are estimated for use in (5).

real-time measurement of a truly gigantic earthquake bearing substantial Pacific-wide tsunami risk, in the $M_m \geq 8.5$ dyn-cm range.

Finally, we wish to emphasize that while this method was being developed, on May 7, 1986, we were able to obtain a correct estimate of $M_0 = 1.0 \times 10^{28}$ dyn-cm for Event 19, within a little more than two hours of the origin time. As a result, no tsunami warning was issued for French Polynesia, and a false alarm avoided [Talandier et al., 1986], while an estimate of tsunami danger based primarily on M_s resulted in the unnecessary evacuation of thousands of residents of Hawaii, Oregon and Washington.

Appendix: Automation of the Measurements

In this section, we discuss briefly an algorithm allowing for automation of the measurement of M_m, which was used to acquire the dataset in Table 1, and is now used routinely by the Polynesian Center for Tsunami Prevention (CPPT) in Tahiti [Talandier and Reymond, 1986]. First, a strong-event detector is triggered, based on the use of the 9 short-period stations of the 350-km aperture Polynesian array continuously telemetered to PPT, and of a classic multiple criterion of amplitude threshold, frequency content, duration and simultaneity. Next, an automated locator uses P times across the array to estimate an epicentral region and an arrival window for R_1. It then triggers acquisition into the computer of 819.2 s at a 0.2 s sampling rate. The computation of M_m then proceeds in two independent ways, providing redundancy of the final results:

Frequency-Domain Measurements.

The time series is simply run through a standard FFT algorithm and the correction C_S applied at each FFT period between 50 s and 300 s. The correction C_D has been regionalized and stored as a function of distance and period for all active epicentral areas of the Pacific region. M_m is then computed from Eqn. (4) at the various periods, and the largest value retained.

Time-Domain Measurements.

The signal is run through a band pass filter eliminating periods outside the 50—300 s range. The resulting time series (see Figure A-1) is searched for subsequent maxima and minima reaching at least 10% of the absolute maximum amplitude of the signal; the resulting amplitudes and periods of the corresponding arches are retained. For each of them, M_m is computed through Eqn. (5), and the maximum value retained.

Acknowledgments. We thank Domenico Giardini for a copy of the Harvard CMT dataset, Barbara Romanowicz for preliminary estimates of M_0, and Otto Nuttli for comments. This research was supported by Commissariat à l'Energie Atomique, and the National Science Foundation, under grant EAR-84-05040.

References

Ekström, G., and A.M. Dziewonski, CMT mechanisms for the Andreanof Islands earthquake sequence [abstract], *Eos, Trans. AGU, 67,* 1082, 1986.

Kanamori, H., The energy release in great earthquakes, *J. Geophys. Res., 82,* 2981-2987, 1977.

Monfret, T., and B. Romanowicz, Importance of on-scale observations of first arriving Rayleigh wavetrains for source studies: Example of the Chile event of March 3, 1985 observed on the Geoscope and IDA networks, *Geophys. Res. Letts., 13,* 1015-1018, 1986.

Okal, E.A., Influence of sediments in tsunami generation [abstract], *Proc. Intl. Tsunami Symposium, Tsunami Comm. Intl. Un. Geod. Geophys.,* Victoria, B.C., Aug. 5-9, 1985, p. 40, 1985.

Okal, E.A., and J. Talandier, M_m: Theory of a variable-period mantle magnitude, *Geophys. Res. Letts., 14,* this issue, 1987.

Shimazaki, K., Nemuro-Oki earthquake of June 17, 1973: A lithospheric rebound at the upper half of the interface, *Phys. Earth Plan. Int., 9,* 314-327, 1974.

Talandier, J., and E.A. Okal, Human perception of T waves: the June 22, 1977 Tonga earthquake felt on Tahiti, *Bull. Seism. Soc. Am., 69,* 1475-1486, 1979.

Talandier, J., and D. Reymond, A new approach for a quick estimation of the seismic moment: Magnitude M_m?, *Proc. Intl. Symp. Natural and Man-made Hazards,* Rimouski, Qué., Aug. 1986, in press, 1986.

Talandier, J., E.A. Okal, and D. Reymond, Mantle magnitude M_m: a new approach for the rapid estimation of seismic moments; application to the 1986 Aleutian earthquake [abstract], *Eos, Trans. AGU, 67,* 1081, 1986.

(Received May 18, 1987;
accepted June 5, 1987.)